Inclusive Deep Inelastic Scattering at HERA and Related Phenomenology

Fabian Zomer

IN2P3-CNRS and Université de Paris-Sud, Laboratoire de l'Accélérateur Linéaire, Bâtiment 200, F-91898 BP 34 Orsay Cedex, France

Abstract. Recent measurements of inclusive deep inelastic scattering differential cross section in the range 1.5 $\mathrm{GeV}^2 \leq Q^2 \leq 30000\ \mathrm{GeV}^2$ and $5 \cdot 10^{-6} \leq x \leq 0.65$ are presented. Phenomenological analyses performed from these measurements are also described.

1 Introduction

In the Deep Inelastic Scattering (DIS) processes observed at HERA, a lepton $\ell = e^{\pm}$ of 27.5 GeV interacts with a proton P of 920 GeV yielding a lepton ℓ' and a set of hadrons X in the final state. Following the nature of ℓ' the interaction proceeds via a neutral ($\ell' = e^{\pm}$) current (NC) or a charged ($\ell' = \nu_e, \bar{\nu}_e$) current (CC). DIS events are collected in the H1 and ZEUS experiments [1] which are located at the two $e^{\pm}P$ interaction points of HERA.

The kinematics of the DIS inclusive processes, $\ell(k) + P(p) \to \ell'(k') + X$, is determined by two independent kinematic variables, besides the energy of the incoming lepton and proton. One usually chooses them among the four Lorentz invariants

$$Q^2 \equiv -q^2 = -(k - k')^2,\ x = \frac{Q^2}{2p \cdot q}\ ,\ y = \frac{p \cdot q}{p \cdot k},\ W^2 = (q + p)^2,$$

whereby at HERA one can neglect the lepton and proton masses so that the useful relation $Q^2 = xys$ holds. These kinematic variables are obtained experimentally by measuring the momentum and/or the hadronic energy, the direction of the scattered lepton and/or the hadronic energy flow.

In this report we shall restrict ourselves to the cross section measurements at HERA in the medium $1.5\ \mathrm{GeV}^2 \leq Q^2 < 150\ \mathrm{GeV}^2$ and high $150\ \mathrm{GeV}^2 \leq Q^2 \leq 30000\ \mathrm{GeV}^2$ domain of the DIS regime. During the past, a large number of precise measurements have been performed in the medium Q^2 region by fixed target experiments [2]. With HERA, three major improvements may be noticed:

- an extension of the Q^2 domain to very high Q^2 ($10^4\ \mathrm{GeV}^2$) but also to very small x ($\approx 10^{-6}$);
- an almost hermetic (4π) detection of the final state leading not only to the determination of the energy and angle of the scattered lepton but also of the produced hadrons;
- from the previous items it follows that the detection of both NC and CC is feasible in the same detector and during the same data taking period;

The somewhat arbitrary distinction between low and high Q^2 is related to different physics interests. In both regions perturbative Quantum-Chromo-Dynamics (pQCD) is expected to describe the HERA data [3]. The pQCD analysis of medium Q^2 data is part of a long tradition [4] from which the parton distributions of the nucleon and the strong coupling constant α_s have been extracted. On the top of that, very high Q^2 ($\approx M_Z^2$) NC and CC data open a field of research in electroweak physics up to now reserved, in DIS, to neutrino beam experiments.

The rest of this report is organized as follows. In section 2 the measurements of NC and CC differential cross sections are described. Section 3 is devoted to a phenomenological analysis of these measurements.

2 Measurement of NC and CC cross sections

Neutral current events, at medium and high Q^2, are basically identified by the presence of an electron (or a positron) in the final state. This is done by using tracking and calorimetric devices covering the range $7^o < \theta_e < 177^o$ and $E'_e > 4$ GeV(at HERA the forward direction $\theta_e = 0^o$ corresponds to the direction of the incoming proton).

The differential cross section measurement is done by counting the number of events within a kinematic interval in, say x and Q^2. Therefore one of the experimental problems is to achieve a good reconstruction of these kinematic variables from the detector information. Both, H1 and ZEUS, can use the outgoing lepton and hadronic final state information, namely the polar angles, the momenta and the deposited energies. It is then possible to define the kinematics of each event by using different (and independent) combinations of experimental information.

In ZEUS the double angle method is used

$$Q^2_{da} = 4E_e^2 \frac{\sin\gamma_h\,(1+\cos\theta_e)}{\sin\gamma_h + \sin\theta_e - \sin(\gamma_h+\theta_e)},\quad y_{da} = \frac{\sin\theta_e\,(1-\cos\gamma_h)}{\sin\gamma_h + \sin\theta_e - \sin(\gamma_h+\theta_e)}$$
$$x_{da} = \frac{E_e}{E_p}\frac{\sin\gamma_h + \sin\theta_e + \sin(\gamma_h+\theta_e)}{\sin\gamma_h + \sin\theta_e - \sin(\gamma_h+\theta_e)}.$$

The hadronic polar angle γ_h is defined by $\tan\gamma_h/2 = \sum_i (E_i - p_{z,i})/P_{t,h}$, where E_i and $p_{z,i}$ are the energy and longitudinal momentum of the final state hadron i and where $P_{t,h}$ is the total transverse momentum of the hadronic final state particles. In H1, the electron method is used

$$Q^2_e = \frac{(E'_e)^2\sin^2\theta_e}{1-y_e},\quad y_e = 1 - \frac{E'_e}{E_e}\sin^2(\theta_e/2)$$

to determine Q^2 and x only at $y > 0.15$ since $dx/x = 1/y dE'_e/E'_e$ while at $y \leq 0.15$ the Σ method is used

$$Q^2_\Sigma = \frac{(E'_e)^2\sin^2\theta_e}{1-y_\Sigma},\quad y_\Sigma = \frac{\sum_i (E_i - p_{z,i})}{\sum_i (E_i - p_{z,i}) + E'_e(1-\cos\theta_e)}.$$

The reason for the differences between the methods used by H1 and ZEUS are related to the calorimeter performances: H1 possesses finely segmented electromagnetic calorimeters and ZEUS a very good hadronic calorimetry.

The redundancy in the determination of the kinematic variables is a crucial point and presents many advantages: minimization of the migration between the 'true' and the measured kinematic variable by choosing one particular method; cross calibration of the various calorimeter devices, and studies of photon radiation from the lepton line by comparing leptonic and hadronic information.

Once the collected events are gathered in x-Q^2 bins, besides the subtraction of photoproduction background, correction factors are applied for: the efficiency of the event selection; detector acceptance; wrong reconstruction of the kinematics due to detector effects, and the contribution of higher order electroweak processes. When possible, these correction factors are determined and/or cross checked from the data themselves. If this is not possible, then they are determined from a full simulation of the DIS and background processes including the detector response.

For the medium Q^2 data we shall describe the preliminary results of the high statistics 1997 data (more than 10000 events per x-Q^2 bin for H1). For high Q^2, the combined 1994-1997 (e^+ beam) data published in ref. [5] are presented.

At medium Q^2 and for the H1 measurements, the main systematic uncertainties are: the electron energy scale ($\approx 0.3\%$), the hadronic energy scale ($\approx 2-3\%$), the electron polar angle (≈ 0.3 mrad), the photoproduction background at high-y only ($\approx 3\%$ effect on the measurements) and the correction factors (see above) applied to the data (each one is of the order of 1-2%). The overall data normalization (including the luminosity measurement) uncertainty is 1.5 %. The systematic uncertainty is, in total, of the order of 3% and is larger than the statistical uncertainties which are at the level of 1 % for $Q^2 < 100$ GeV^2.

At high Q^2 the systematic uncertainties are essentially the same. In ZEUS the statistic and systematic uncertainties amount to 3-5% for the kinematic range 400 GeV$^2 < Q^2 < 30000$ GeV^2 considered in the analysis.

In charged current events, the outgoing neutrino escapes the detection. Such events are then characterized by missing transverse energy $p_{t,miss}$ Analysis in ZEUS (H1) have demanded $p_{t,miss} > 10$ GeV ($p_{t,miss} > 12$ GeV). For the reconstruction of the kinematic variables, one can only use information from the hadronic final state, i.e. the Jacquet-Blondel method, giving,

$$y_{JB} = \frac{\sum_i (E_i - p_{z,i})}{2E_e}, \;\; Q^2_{JB} = \frac{p^2_{t,miss}}{1 - y_{JB}}.$$

The CC events statistics is still low, ≈ 900 events for $Q^2 > 400$ GeV^2 in ZEUS. The systematic uncertainty is dominated by the hadronic energy scale, which induces an effect of the order of 10%, except at very high Q^2 and very high x where the effect is above 20%. Other systematic sources related to the $p_{t,miss}$ cut, acceptance correction and photoproduction background subtraction (in the lowest Q^2 bins) lead to measurement uncertainties between 4% and 8%.

3 Phenomenological analysis of inclusive measurements at HERA

As mentioned in the introduction, we shall distinguish the phenomenological analysis of the medium Q^2 data from the high Q^2 data. As we are interested in the HERA data, it should be noted that we are considering the region of large $W^2 \gg 10$ GeV^2. Therefore, we will not be concerned by the non-perturbative effects and the higher twist effects appearing in this region so that the symbol pQCD, appearing below, refers to the leading twist of pQCD.

For all the mathematical details which cannot be given here we refer to ref. [6] and references therein.

3.1 Analysis of the medium Q^2 NC data

In the one boson exchange approximation, the NC differential cross section reads

$$\frac{d\sigma^{e^{\pm}p}}{dxdQ^2} = \frac{2\pi\alpha_{em}Y_+}{xQ^4}\sigma_r, \;\; \sigma_r = F_2(x,Q^2) - \frac{y^2}{Y_+}F_L(x,Q^2) \mp \frac{Y_-}{Y_+}xF_3(x,Q^2)\,, \quad (1)$$

where $Y_\pm = 1 \pm (1-y)^2$. The nucleon structure functions are modeled using the quark-parton model and pQCD. In the so called naive parton model one writes

$$F_2(x) = \sum_{i=1}^{n_f} A_i(Q^2)x[q_i(x) + \bar{q}_i(x)]\,,\; F_3(x) = \sum_{i=1}^{n_f} B_i(Q^2)[q_i(x) - \bar{q}_i(x)]$$

where q_i ($\bar{q}_i$)is the density function of the quark (anti-quark) of flavor i, n_f is the number of active flavors and $F_L = 0$. The functions A_i [4] depend on the electric charge e_i ($A_i = e_i^2$ for $Q^2 \ll M_Z^2$) and embody the effects of the Z exchange and $\gamma - Z$ interference in their Q^2 dependence. The same holds for the functions B_i [4] except that they vanish at $Q^2 \ll M_Z^2$.

Going beyond the simple parton model, higher order contributions in α_s are taken into account. However mass singularities appear in the initial state of DIS processes and cannot be regularised without resumming the whole perturbative series. This resummation is done in a restricted kinematic region where $\alpha_s \log Q^2$ is large [6]. This latter region is defined by $Q^2 \gg \Lambda^2 \approx 0.3^2$ GeV^2, and the pQCD calculations are safe for Q^2 above a few GeV^2. In this domain, the parton density functions (pdf) are given by the solution of the DGLAP equations [6]:

$$\begin{aligned} M_F\frac{\partial q^{\pm}_{i,NS}(x,M_F^2)}{\partial M_F} &= P^{\pm}_{NS} \otimes q^{\pm}_{i,NS}(x,M_F^2) \\ M_F\frac{\partial}{\partial M_F}\begin{pmatrix}\Sigma(x,M_F^2)\\ g(x,M_F^2)\end{pmatrix} &= \begin{pmatrix}P_{qq} & n_f P_{qg}\\ P_{gq} & P_{gg}\end{pmatrix} \otimes \begin{pmatrix}\Sigma(x,M_F^2)\\ g(x,M_F^2)\end{pmatrix} \end{aligned} \quad (2)$$

with $A \otimes B \equiv \int_x^1 A(z)B(x/z)dz/z$ and where $\Sigma = \sum_{i=1}^{n_f}(q_i + \bar{q}_i)$ is the singlet quark density, $q^-_{i,NS} = q_i^v \equiv q_i - \bar{q}_i$ and $q^+_{i,NS} = q_i + \bar{q}_i - \Sigma/n_f$ are the two

non singlet densities and g is the gluon density. The splitting functions $P_{i,j} = \alpha_s(M_R^2)P_{i,j}^{(0)} + \alpha_s^2(M_R^2)P_{i,j}^{(1)}$ describe the branching of parton j from parton i, and they can be computed with pQCD up to the second order. In eq. (2) M_F is the factorization scale (below which the mass singularity is resummed) and M_R is the renormalisation scale (related to the ultra-violet singularity). As the two scales must be chosen somehow, a natural choice for M_F is $\sqrt{Q^2}$, i.e. the virtual mass of the probe. We shall, as usual, also set $M_R = M_F$ for convenience. It is worth mentioning that the DGLAP equations are universal, i.e. that they are independent of the specific hard process.

Eq. (2) embodies the mass singularity resummation and therefore it only describes the so called light parton, i.e. the parton of flavour i and mass m_i such that $m_i^2/Q^2 \ll 1$. In the medium Q^2 range one can take the gluon, the up, down and strange quarks as the light partons. For the heavy quarks (charm and beauty) one needs to specify a special scheme. We have chosen the fixed-flavor-scheme (FFS) [7] – suitable in the HERA medium Q^2 range – where beauty is neglected, and where the charm contribution is computed from the boson-gluon-fusion process $\gamma g \to c\bar{c}$ plus the α_s^2 corrections. In this scheme charm is produced 'outside' the hadron. The relation between the pdfs and the structure functions depends on the renormalisation scheme. In Next-to-Leading-Log-Approximation (NLLA) and in the $\overline{\text{MS}}$ scheme one obtains:

$$F_i(x,Q^2) = x\sum_{j=1}^{n_f}\left[\left(1+\frac{\alpha_s(Q^2)}{2\pi}C_{j,q}\right)\otimes e_j^2(q_j(x,Q^2)+\bar{q}_j(x,Q^2)) + 2\frac{\alpha_s(Q^2)}{2\pi}C_{j,g}\otimes g\right] + F_i^{c\bar{c}}(x,Q^2)$$

for $n_f = 3$ and where $i = 1, 2$ (there is a similar expression for F_3 with $F_3^{c\bar{c}} = 0$); $C_{j,q}$ and $C_{j,g}$ are the coefficient functions depending on the hard process; $F_i^{c\bar{c}}$ is the charm contribution [8]. It suffices here to say that it depends on m_c^2 and on a renormalisation scale that we choose to be $\sqrt{m_c^2+Q^2}$. Note that $F_L = F_2 - 2xF_1 \neq 0$ in the NNLA.

To solve the system of integro-differential equations (2), one must provide some initial conditions, i.e. some input functions of x at a given Q^2 for each pdf. Since these functions reflect some unknown non-perturbative mechanism, one must parameterize with the help of a set of parameters. As we shall see below, these parameters are determined by comparing the calculations to the experimental data. However, the inclusive DIS data alone cannot constrain all light flavours since the structure functions are linear combinations of the pdfs: introducing the singlet and a non-singlet $xu^+ = xu + x\bar{u} - x\Sigma/3$ densities in order to write $\sum_{i=1}^{n_f=3} e_i^2 x[q_i(x,Q^2)+\bar{q}_i(x,Q^2)] = 2/3xu^+ + 1/9x\Sigma$. There is one important property of the DGLAP kernels $P_{i,j}$: the average total momentum carried by the partons, $\int_0^1(x\Sigma + xg)dx$, is independent of Q^2. This quantity is called the momentum sum rule and is usually fixed to 1.

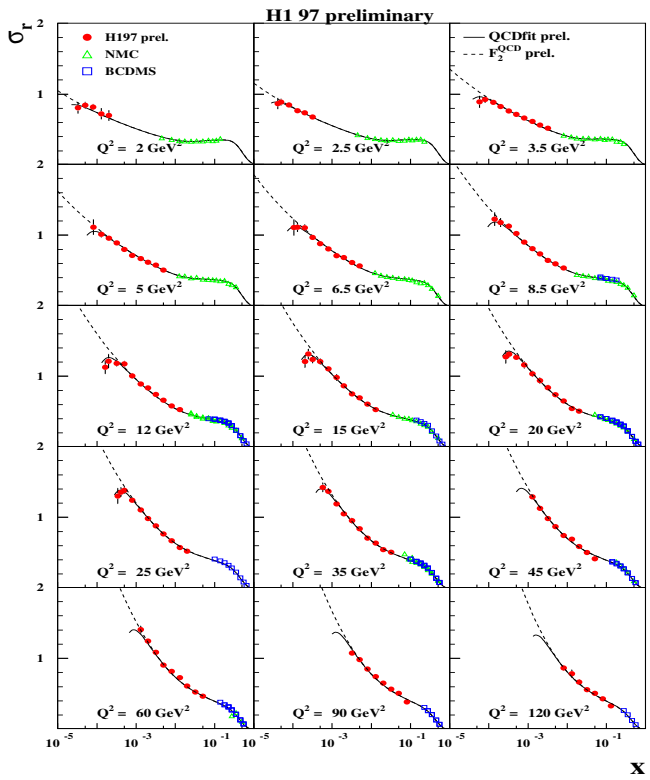

Fig. 1. H1 preliminary measurements of σ_r together with the result of a pQCD fit (see text).

So in principle one may be able to describe the inclusive HERA data by parameterizing the three functions xg, $x\Sigma$ and xu^+. But we found that such a description is not adequate for the following reasons:

- it leads systematically to a too large fraction of the total momentum carried by the gluons $\int_0^1 xgdx > 60\%$, in contradiction with the results of global fits including specific constrain on xg at high x [9];
- since the DGLAP equations involve some integrals of the pdfs from x to 1, one must also introduce some constraints at higher x, i.e. the fixed target hydrogen data from NMC and BCDMS [2];
- even when fixed target hydrogen data are included, one is unable to constrain the total momentum carried by the gluons. One must in addition include the fixed target deuterium data. In this case a second non-singlet density must be parameterized (essentially $u + \bar{u} - d - \bar{d}$), but now the valence counting rules, $\int_0^1 (u - \bar{u})dx = 2$ and $\int_0^1 (d - \bar{d})dx = 1$, can be applied, under certain assumptions, in order to constrain the momentum sum rule at high x.

H1 and ZEUS have used the latter option but with different assumptions. We will describe here the fits performed to the 1994 data and to the preliminary 1997 data. Both experiments include their own inclusive measurements and the NMC and BCDMS data.

In H1 two assumptions are made: $\bar{u} = \bar{d}$ and $\bar{s} = s = \bar{d}/2$. The first constraint is in contradiction with the global fit results [9] including the Drell-Yan data but we have found that it does not modify significantly the gluon density at below $x \approx 10^{-2}$. The second assumption comes from the results of the dimuon events of CCFR [10]. Finally xg, $x\bar{u}$, xu_v and xd_v are parameterized at a given value of Q^2 using the mathematical function $Ax^B(1-x)^C P(x)$ with $P(x) = 1 + Dx + E\sqrt{x}$. The momentum sum-rule and the quark counting rules are applied so that there are 16 free parameters in the H1 fit.

In ZEUS, the two valence quarks are taken from the MRS parameterization [9] and $\bar{s} = s = (\bar{d} + \bar{u})/2$ is also applied. xg, $x(\bar{u} - \bar{d})$ and $x(\bar{u} + \bar{d})$ are parameterized using the above mathematical functions.

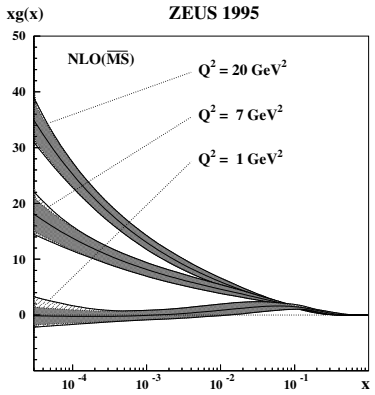

Fig. 2. xg extracted from the ZEUS fit to the 1994 data for three values of Q^2. Error bands contain the experimental error propagation and a theoretical error estimation (see text).

Concerning the data-theory comparison, from which the input pdfs have to be determined, both H1 and ZEUS use a χ^2 minimization procedure. The main steps of the fitting procedure are summarized below. For each iteration: 1) the pdf's are parameterized at a given value of Q^2 denoted Q_0^2, it is chosen to be 7 GeV^2 in the ZEUS fit and 4 GeV^2 in the H1 fit, 2) the DGLAP equations are solved numerically in x-space [11]. 3) the evolved pdf's are convoluted with the coefficient functions to obtain the structure functions. Assuming that all experimental uncertainties are normally distributed a χ^2 is computed. A crucial point of the analysis is the χ^2 expression which permits the use of the correlations

introduced by some of the systematic uncertainties:

$$\chi^2 = \sum_{exp}\sum_{dat} \frac{[\mathcal{O}^{dat}_{exp} - \mathcal{O}^{fit} \times (1 - \nu_{exp}\sigma_{exp} - \sum_k \delta^{dat}_k(s^{exp}_k))]^2}{\sigma^2_{dat,stat} + \sigma^2_{dat,uncor}} + \sum_{exp} \nu^2_{exp} + \sum_{exp}\sum_k (s^{exp}_k)^2$$

where $\mathcal{O}$ stands for the observables (structure functions and differential cross

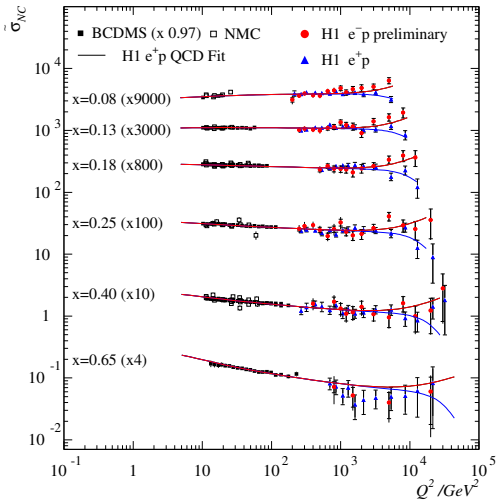

Fig. 3. High Q^2 H1 measurements of $\tilde{\sigma} \equiv \sigma_r$ (eq. 1) compared with pQCD fit results (see text).

sections). The first two sums run over the data (dat) of the various experiments (exp); σ_{exp} is the relative overall normalization uncertainty of the experiment exp; $\sigma_{dat,stat}$ and $\sigma_{dat,uncor}$ are the statistical error and the uncorrelated systematic error, respectively, corresponding to the data point dat; ν_{exp} is the number of standard deviations corresponding to the overall normalization of the experimental sample exp; $\delta^{dat}_k(s^{exp}_k)$ is the relative shift of the data point dat induced by a change by s^{exp}_k standard deviations of the k^{th} correlated systematic uncertainty source of the experiment exp. It is estimated by

$$\delta^{dat}_k(s^{exp}_k) = \frac{\mathcal{O}^{dat}_{exp}(s^{exp}_k = +1) - \mathcal{O}^{dat}_{exp}(s^{exp}_k = -1)}{2\mathcal{O}^{dat}_{exp}} s^{exp}_k + \left[\frac{\mathcal{O}^{dat}_{exp}(s^{exp}_k = +1) + \mathcal{O}^{dat}_{exp}(s^{exp}_k = -1)}{2\mathcal{O}^{dat}_{exp}} - 1\right](s^{exp}_k)^2 ,$$

where $\mathcal{O}_{exp}^{dat}(s_k^{exp} = \pm 1)$ is the experimental determination of $\mathcal{O}_{exp}^{dat}$ obtained varying by $\pm 1\sigma$ the k^{th} source of uncertainty. Parameters ν_{exp} and s_k^{exp} can be determined by the χ^2 minimization or they can be fixed to zero during the minimization but released during the χ^2 error matrix calculation. In the first case one uses all the experimental information relying on the correctness of the estimate of the systematic uncertainties.

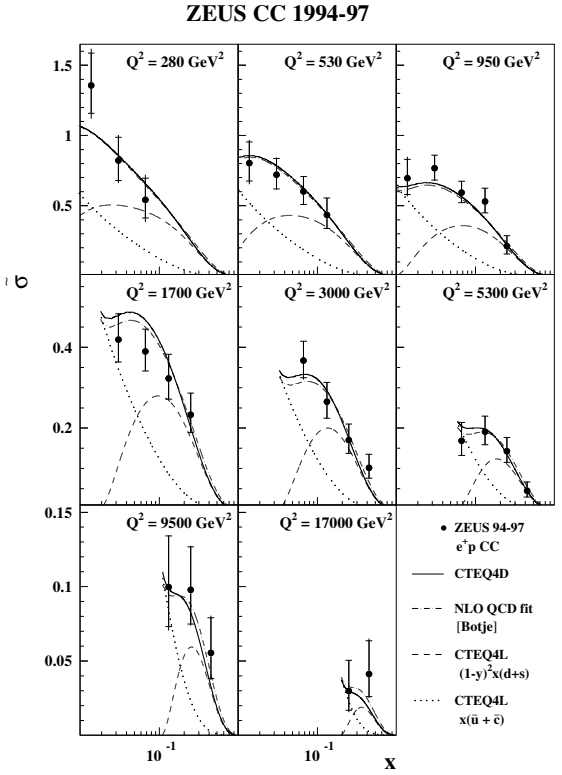

Fig. 4. ZEUS measurements of $\tilde{\sigma} \equiv \Phi_+$ together with various pQCD calculations (see text).

The result of the H1 fit is shown in fig. 1 together with the data. The agreement between data and pQCD is excellent. The gluon density obtained from the ZEUS fit (to the 1994 data) is shown in fig. 2. The error bands of the gluon density include the experimental error propagation as defined in ref. [12] and a theoretical uncertainty which includes the variation of: α_s, the charm mass, the pdf input parameterization form, the value of Q_0^2 and the factorization scale. With the 1997 data one can expect a reduction of the experimental uncertainty by a factor of two. The theoretical uncertainties will then dominate in the determination of xg, i.e. the third order splitting functions are needed.

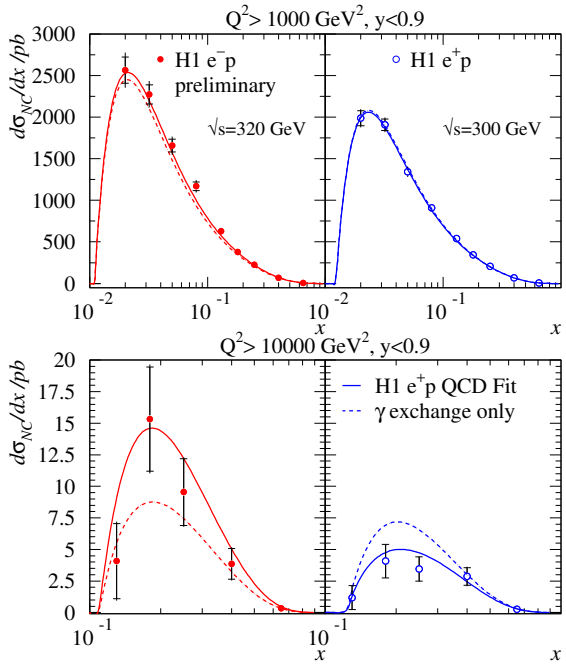

Fig. 5. H1 measurements of $d\sigma^{NC}/dx$ together with results from pQCD fits and different assumptions on electroweak contributions (see text).

3.2 Analysis of the high Q^2 NC and CC data

The fits applied to the high Q^2 data differ from the one described in the previous section by a different calculation of the contribution of the heavy quarks to the structure functions. As $m_c \approx 1.5$ GeV, one has $m_c/Q^2 \ll 1$ at high Q^2. The large term $\alpha_s^n \log^n(Q^2/m_c^2)$ – dominating the calculation of $F_2^{c\bar{c}}$ – must be resummed already at $Q^2 \approx 20$ GeV^2. The massless scheme is therefore used and only data with $Q^2 \geq 10$ GeV^2 are included in the fit. In the massless scheme, charm and beauty are considered as partonic constituents of the proton and their density functions are obtained by solving the DGLAP equations with the initial conditions $c(x, Q^2 \leq m_c^2) = 0$ and $b(x, Q^2 \leq m_b^2) = 0$. Such fits describe the HERA NC and CC (see fig. 3 and 4) data above $Q^2 = 10$ GeV^2.

In fig. 3 one can observe the different behavior of e^-p and e^+p cross sections at very high Q^2. This is related to the different sign of the contributions of F_3 to σ_r. Fig. 5 shows $d\sigma/dx$ together with the results of two pQCD fits including or not the Z exchange and $\gamma - Z$ interference. With the present data, sensitivity to electroweak effects in NC is for the first time observed at HERA.

Up to now we have only described the NC cross sections and related structure functions. For CC processes, in the one boson exchange approximation, one has

$$\frac{d\sigma_{CC}^{e^{\pm}p}}{dxdQ^2} = \frac{G_F^2}{2\pi x}\frac{M_W^4}{(M_W^2+Q^2)^2}\Phi_{\pm}(x,Q^2), \tag{3}$$

where G_F is the Fermi constant, and where the functions $\Phi_{\pm}$ depends on CC structure functions (see [4] for example). From eq. (3) one can first remark that the Q^2 slope of the CC differential cross section (see fig. 6) permits a

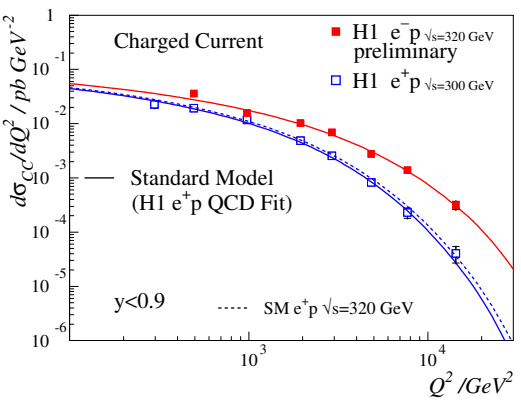

Fig. 6. H1 measurements of $d\sigma^{CC}/dQ^2$ together with the pQCD fit results.

determination of M_W, assuming (or not) the precisely measured value for G_F [13]. To extract M_W, H1 and ZEUS have used two different procedures. In H1, M_W is taken as an extra free parameter (G_F is fixed) of the pQCD fit and in ZEUS, the pdfs of CTEQ [9] are used in order to extract M_W and G_F (variations of the pdf choice is taken into account within the errors). The results are

$$\text{H1}: \mathrm{M_W} = 80.9 \pm 3.3(stat.) \pm 1.7(syst.) \pm 3.7(theo)\,\mathrm{GeV}$$
$$\text{ZEUS}: \mathrm{M_W} = 80.4^{+4.9}_{-2.6}(stat.)^{+2.7}_{-2.0}(syst.)^{+3.3}_{-3.0}(pdf)\,\mathrm{GeV}$$

and treating G_F as free, ZEUS obtain

$$M_W = 80.8^{+4.9}_{-4.5}(stat.)^{+5.0}_{-4.3}(syst.)^{+1.4}_{-1.3}(pdf)\,\mathrm{GeV},$$
$$G_F = [1.171 \pm 0.034(stat.)^{+0.026}_{-0.032}(syst.)^{+0.016}_{-0.015}(pdf)] \times 5 \cdot 10^{-5}\,\mathrm{GeV}^{-2}.$$

Let us point out that, concerning the H1 result, the theoretical uncertainty is dominated by the variation of the results when varying the ratio $\bar{d}/\bar{u}$ in the pQCD fit, and by the choice of the nuclear corrections applied to the deuterium target data entering the fit. These results, in good agreement with the world average values [13], show that the standard model gives a good description of both

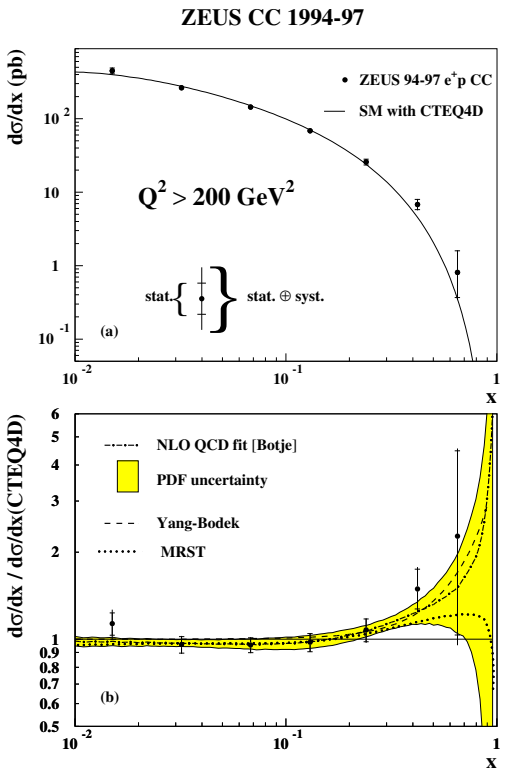

Fig. 7. ZEUS measurements of $d\sigma^{CC}/dx$ (for e^+p) together with various pQCD results (see text).

space-like (CC in DIS) and time-like (W production in $p\bar{p}$ and e^+e^- collisions) processes.

In order to see the sensitivity of the CC cross section to the pdfs, we write $\Phi_\pm$ in LO

$$\Phi_+ = x\bar{U} + (1-y)xD; \;\; \Phi_- = xU + (1-y)x\bar{D}$$

with $U = u + c$ and $D = d + s$. From these expressions and from fig. 4 one can remark that: with positron (electron) beams one can determine d^v (u^v) at high x and small-y and $\bar{u} + \bar{c}$ ($\bar{d} + \bar{s}$) at small y. Let us mention that d_v and the sea quarks are basically determined in the global pQCD fits by μd and $\nu(\bar{\nu})F_e$ fixed target data, which require some nuclear corrections. Therefore, with the HERA $e^\pm p$ CC events one may have, with more statistics, a unique means to determine properly these quark densities.

In fig. 7, $d\sigma/dx$ is shown together with the error band determined by the ZEUS pQCD fit (without the CC and NC data described in the present article), and with the results of a recent analysis where an ansatz $d/u \neq 0$ as $x \to 1$ [14]

was introduced. Although the statistics is still low, one can notice from fig. 7 that this latter hypothesis is not required by the HERA data.

In fig. 8, the preliminary 1998 measurement of $d\sigma^{e^-p}/dx$ is shown. The error

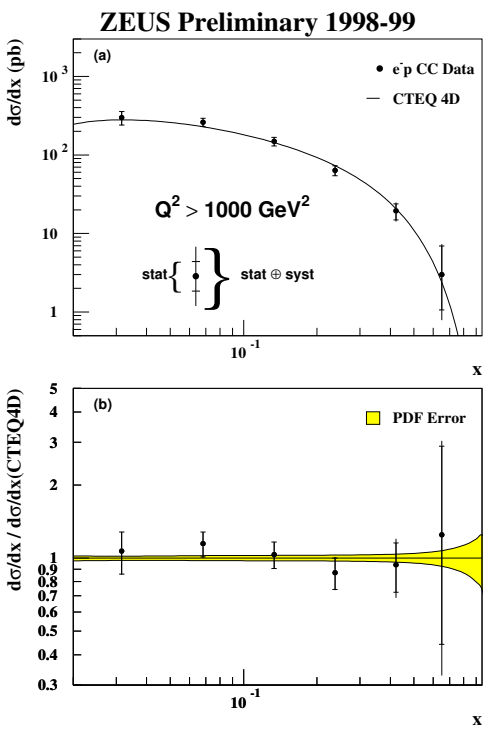

Fig. 8. ZEUS measurements of $d\sigma^{CC}/dx$ (for e^-p) together with the pQCD fit result.

band of the pQCD is much smaller than in fig. 7, therefore one can expect a better determination of electroweak parameters. The size of the error bands reflect that u^v is much better constrained than d^v in the pQCD fits.

3.3 Extraction of F_L

The longitudinal structure function is very hard to determine. It requires to combine data in a given x-Q^2 bin from different beam energies. However, from eq. (1), one observes that at high y the cross section receives a contribution both from F_2 and F_L. Therefore, taking F_2 from the result of a pQCD fit (see previous section) applied to the low y ($y < 0.35$) data one can determine F_L at high y by subtracting F_2, extrapolated to high y. The result of this operation is shown in

fig. 9. To reach lower Q^2, where pQCD is not reliable, another method is used. Writing

$$\frac{\partial \sigma_r}{\partial \log y} = \frac{\partial F_2}{\partial \log y} - 2y^2 \frac{2-y}{Y_+^2} F_L - \frac{y^2}{Y_+} \frac{\partial F_L}{\partial \log y},$$

neglecting $\partial F_L / \partial \log y$, and assuming that $\partial F_2 / \partial \log y$ is a linear function of $\log y$, one obtains the results also shown in fig. (9). This determination is consistent with the LO calculation of pQCD.

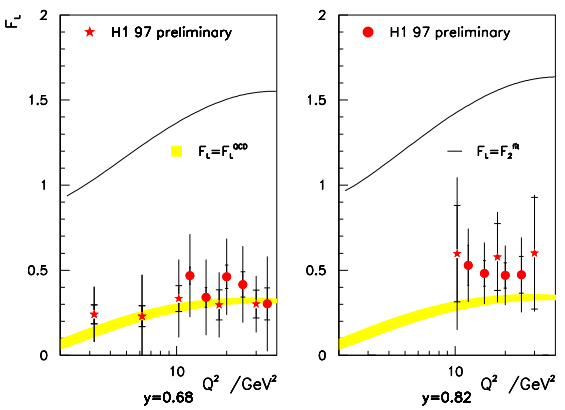

Fig. 9. H1 determination of F_L. The full points correspond to the subtraction method and the stars to the derivative method (see text).

4 Conclusion

Recent measurements of medium and high Q^2 differential cross sections at HERA have been presented, and a determination of F_L was also described. These new inclusive DIS data cover four orders of magnitude in Q^2 and five orders of magnitude in x.

In order to test Quantum Chromodynamics, fits based on the DGLAP equations have been performed successfully to the NC and CC data sets presented in this article. The extraction of the gluon density was described and the result of the analysis of the 1994 data was shown.

At medium Q^2 HERA has reached the limit where the systematic uncertainties dominate the statistical ones. With the 1997 data, the gluon density will be determined by the pQCD fit at the few percent level of accuracy, and a determination of both xg and α_s, is now foreseen.

Concerning the high Q^2 data, although the statistics of NC and CC events is still low, a sensitivity of the results to the effects of Z boson and $\gamma - Z$ interference in NC and to M_W in CC was observed. A determination of M_W from

$d\sigma^{CC}/dQ^2$ in space-like DIS was reported and a good agreement was found with the world average value from measurements in the time-like regions. Furthermore, comparing $d\sigma^{CC}/dxdQ^2$ with the pQCD calculation, we pointed out that such a measurement offers a unique possibility to pin down – independently of any nuclear effects – d^v and the different components of the proton sea.

Finally, comparing the measurements of $d\sigma^{e^+p}/dxdQ^2$ and $d\sigma^{e^-p}/dQ^2$ we observed, for the first time, the sensitivity of the NC to F_3.

With the high Q^2 NC and CC events a new field of research is touched here. It will be covered, with more precision, by the HERA-2000 upgrade with the help of an increase of luminosity and longitudinal polarization of the lepton beam.

References

1. H1 Coll., Nucl. Instr. Meth A336, **310** and **348** (1997); The ZEUS detector, status report DESY-1993.
2. BCDMS Coll., Phys. Lett. B223, **485** (1989); Phys. Lett. B237, **592** (1989); NMC Coll., Nucl. Phys. B**483**, **3** (1997).
3. H1 Coll. Nucl. Phys. B470, **3** (1996); ZEUS Coll. Eur. Phys. J. C7, **609** (1999), see also M. Botje, DESY 99-038 for the ZEUS pQCD fits.
4. See for a recent review: A.M. Cooper-Sarkar, R.C. Devenish and A. De Roeck, Int. J. Mod. Phys. A13, **3385** (1998).
5. H1 Coll., DESY 99-107; ZEUS Coll., DESY 99-56 and DESY 99-59.
6. W. Furmanski and R. Petronzio, Z. Phys. C1, **293** (1982).
7. M. Glück, E. Reya and M. Stratmann, Nucl. Phys. B422, **37** (1994).
8. E. Laenen et al., Nucl. Phys. B392, **162** and **229** (1993); Phys. Lett. B291, **325** (1992).
9. CTEQ4 Coll., Phys. Rev. D55, **1280** (1997); MRS Coll., Phys. Rev. D51, **4756** (1995).
10. CCFR Coll., Z. Phys. C65, **189** (1995).
11. C. Pascaud and F. Zomer, DESY 96-266; J. Blümlein et al., in Proc. of the Workshop on Future Physics at HERA, G. Ingelman, A. De Roeck and R. Klanner eds., **23** DESY (1996).
12. C. Pascaud and F. Zomer, LAL 95-05.
13. Particle Data Group, Eur. Phys. J. C3, **1** (1998).
14. U.K. Yang and A. Bodek, Phys. Rev. Lett. 82, **2467** (1999).
15. See for instance Proc. of the Workshop on Future Physics at HERA, G. Ingelman, A. De Roeck and R. Klanner eds., DESY (1996).